한국해양공학회지 제25권 제6호, pp 1-8, 2011년 12월 (ISSN 1225-0767)

Development of Digital Gas Metal Arc Welding System and Welding Current Control Using Self-tuning Fuzzy PID

Phuc Thinh Doan*, Pandu Sandi Pratama*, Suk Yoel Kim*, Hak Kyeong Kim*, Hwang Yeong Yeun**, Gi Sig Byun** and Sang Bong Kim*

*Department of Mechanical Eng., College of Eng., Pukyong National University

**Department of Control and Instrumentation Eng., College of Eng., Pukyong National University

KEY WORDS: GMAW, Gas Metal Arc Welding, Fuzzy, PID controller

ABSTRACT: *This paper describes a new method for a digital gas metal arc welding (GMAW) system. The GMAW system is an arc welding process that incorporates the GMAW power source (PS-GMAW) with a wire feed unit (WFU). The PS-GMAW requires an electric power of constant voltage. A constant magnitude is maintained for the arc current by controlling the wire-feed speed of the WFU. A mathematical model is derived, and a self-tuning fuzzy proportional-integral-derivative (PID) controller is designed and applied to control the welding current. The electrode wire feeding mechanism with this controller is driven by a DC motor, which can compensate for both the molten part of the electrode and undesirable fluctuations in the arc length during the welding process. By accurately maintaining the output welding current and welding voltage at constant values during the welding process, excellent welding results can be obtained. Simulation and experimental results are shown to prove the effectiveness of the proposed controller.*

1. Introduction

Arc welding is one of the key processes in industrial manufacturing such as the automotive, ship building, and construction industries. Among the various types of weldin GMAW is extensively used because of its high speed and suitability for both manual and automatic modes of welding for a wide range of ferrous and nonferrous metal parts (Kam et al., 2002; Naidu et al., 2003).

Both arc voltage and welding current are mainly controllable parameters in GMAW process. Many qualitative features of welding are affected by process parameters such as weld geometry, weld metallurgical characteristics, transfer mode of melting droplets, weld stability, weld defects, and strength (Mohammad and Mohammad 2011). Some control approaches have been introduced to control these variables. Naidu et al. (2003) designed two PI controllers to control the process. Abdelrahman (1998) used feedback linearization to control the current and arc length in the GMAW system. However, those methods have limitations because of the nonlinear characteristics and inaccuracies of the GMAW process model. Ngo et al. (2007) applied a sliding mode to control the wire-feeding rate to obtain a desired constant welding current. The adaptive control was also implemented to design the adaptive predictive control system for welding process by Zhang and Liu (2003). Another method was introduced by Mohammad and Mohammad (2011), who used an ARMarkov-based MPC to control the welding current and arc voltage with uncertainties in the linearized GMAW model, along with the system parameters. However, their studies usually required large time-consuming calculations.

To overcome the above problem, various GMAW systems have been developed. Because of the revolution in integrated circuit technology, which now permits high quality, small, quick response circuits, it is reasonable to use an IC in the design of PS-GMAW. The PS-GMAW controller incorporates both a microcontroller and IC TL494. The PS-GMAW is a constant voltage power supply. Most gas metal arc welding systems use a constant voltage power supply because of their ability to self-regulate the arc length (Naidu et al., 2003). Furthermore, a constant welding current is achieved by controlling the wire-feed speed. It is possible to use a conventional PID to control the wire-feed speed of the WFU. However, conventional PID controllers do not yield reasonable performance over a wide range of operating conditions because of the fixed gains used. Thus, the PID parameters need to be automatically adjusted by a fuzzy set (Truong and Aha, 2009).

This paper presents a new closed-loop control method based on a self-tuning fuzzy PID controller. The developed digital GMAW system permits the output welding current and voltage to track any set values easily and quickly. The developed GMAW system allows welding voltage settings of 16 VDC to 36 VDC and welding currents from 50 A to 220 A. The simulation and experimental results are shown to prove the effectiveness of the proposed system and controllers.

Corresponding author Sang Bong Kim: 365, Sinseon-ro, Nam-Gu, Busan, Korea, +82-51-629-6158, kimsb@pknu.ac.kr.

2. System description and principles of operation

Fig. 1 shows the configuration of fundamental equipments necessary for the GMAW system. The wire feed speed of the WFU has a range of about 1.9 to 30 m/min. It consists of a DC motor, gearbox, guide tube clamp, and feed rolls. The welding electrode wire is fed by the WFU to compensate for the electrode melting-rate in order to continuously maintain a welding arc during the welding process. The variable electrode feed-rate makes the output welding current change. The WFU must be controlled in order to achieve the set welding current and obtain a clean positive arc with each strike. Furthermore, it must minimize stubbing, skipping, and spatter, and also maintain steady wire feeding during the welding process.

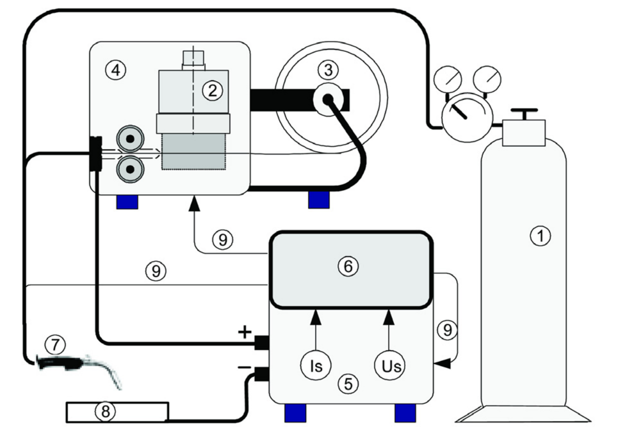

Fig. 1 Configuration of fundamental equipments necessary for GMAW system: (1) shielding gas; (2) DC motor and gear box; (3) welding electrode roll; (4) WFU; (5) PS-GMAW; (6) control box; (7) welding gun; (8) workpiece; (9) control cable

To clearly illustrate this concept, Fig. 2 shows the relationship between the welding current and electrode feed-rate (Lincoln Electric Company, 1997) for an aluminum wire positive electrode.

The PS-GMAW is a constant voltage power supply. As a result, any change in arc length (which is directly related to voltage) results in a large change in heat input and current. A shorter arc length produces a greater heat input. This makes the wire electrode melt more quickly and thereby restores the original arc length. This helps operators keep the arc length constant. This effect has been called self regulation. Fig. 3 shows the volt-ampere characteristics of a typical constant-voltage power supply, along with the arc voltage curves (Naidu et al., 2003).

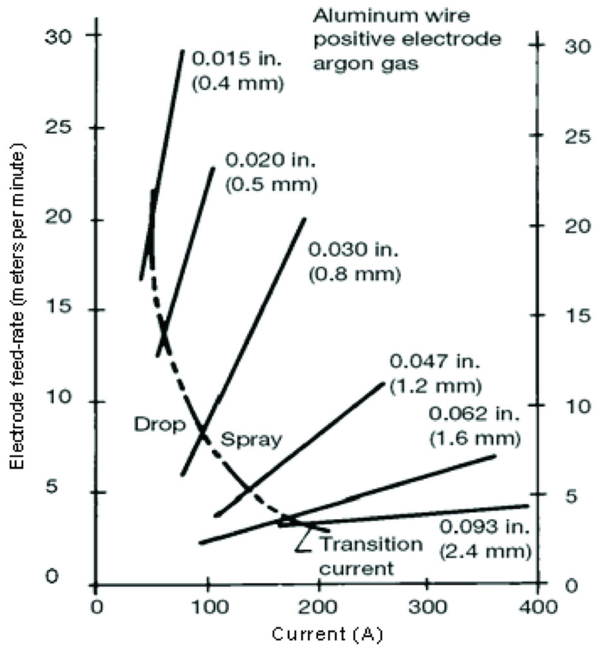

Fig. 2 Relationship between the electrode feed-rate and welding current

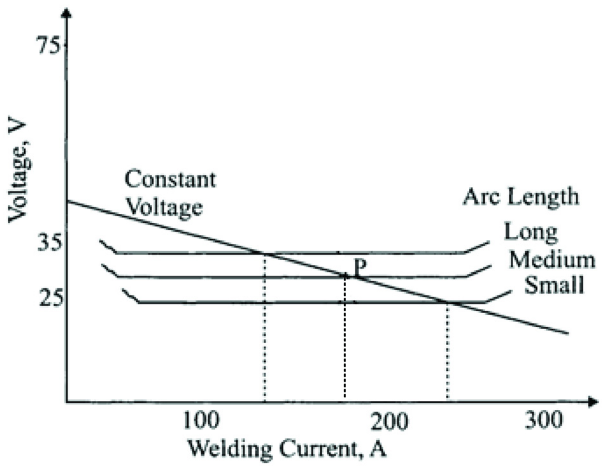

Fig. 3 Self-regulation of arc voltage

3. PS-GMAW design

Fig. 4 explains the typical block diagram of the PS-GMAW used for the GMAW system (American Welding Society Inc., 1997). The incoming three-phase or single phase 50/60 Hz, AC power is converted into DC by the full wave rectifier. This DC is applied to the inverter using semiconductor switches, and the inverter inverts the DC into high-frequency square wave AC. This high-frequency voltage allows the use of a smaller step down transformer. After being transformed, the AC is rectified to DC for welding.

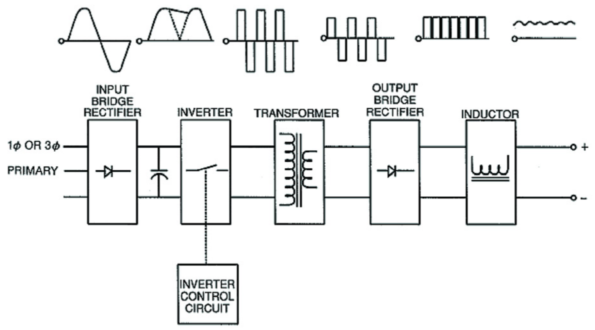

Fig. 4 Block diagram of PS-GMAW

The PS-GMAW schematic is shown in Fig. 5. The controller incorporates both a microcontroller and IC TL494. The TL494 is a single monolithic chip designed for power supply control. The microcontroller is connected to a user interface so that welders can set all of the parameters for welding such as the welding wire diameter, protection gas mixture, and welding voltage.

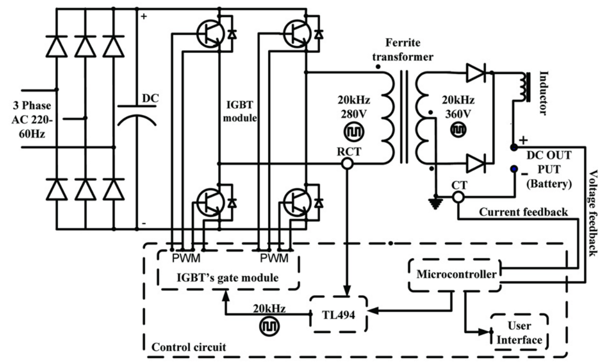

Fig. 5 Schematic circuit of PS-GMAW

4. WFU controller design

4.1 Model of WFU

In this system, a DC servomotor is utilized to control the DC motor of the WFU, which controls the electrode feed-rate to maintain the welding arc. The dynamic relationship between the electrode feed-rate and the voltage applied to the DC motor of the WFU can be expressed as a second-order dynamic equation as follows:

$$G_m(s) = \frac{W_f(s)}{V_m(s)} = \frac{b_0}{s^2 + a_1 s + a_0} \tag{1}$$

where $W_f(s)$ and $V_m(s)$ represent the electrode feed-rate and DC voltage applied to the DC motor of the WFU, respectively.

The purpose of controlling the WFU is to change the electrode feed-rate to track the set value, I_s. In the GMAW process, the electrode feed-rate must be equal to the electrode melting-rate to maintain a stable arc length.

$$W_f = W_m \tag{2}$$

where W_m is the electrode melting-rate.

The electrode melting-rate, W_m, can be expressed as a function of welding current, I_w, and welding voltage, U_w, as follows (Chu and Tung 2005; Ngo et al., 2007):

$$W_m = K_c I_w - K_v U_w \tag{3}$$

where K_c and K_v are the coefficient ratios of the melting- rate to the welding current and welding voltage, respectively.

From Eqs. (2) and (3), the electrode feed-rate can be expressed as:

$$W_f(s) = K_c I_w - K_v U_w \tag{4}$$

Therefore, the welding current can be expressed as:

$$I_w = \frac{W_f(s)}{K_c} + \frac{K_v U_w}{K_c} = \frac{W_f(s)}{K_c} + \frac{\Delta G}{K_c} \tag{5}$$

where $\triangle G$ denotes $K_v U_w$.

In fact, the welding current influences the electrode feed-rate much more than does the welding voltage. If the welding voltage is considered as a disturbance in Eq. (4), the block diagram for an open loop transfer function of the WFU is shown in Fig. 6.

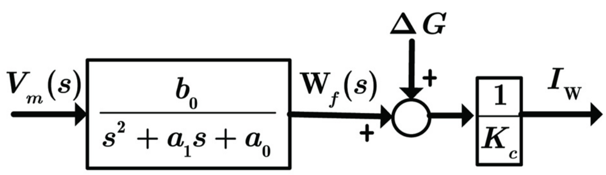

Fig. 6 Block diagram of open loop of WFU

If $\triangle G$ is considered to be a disturbance of the system, from Eqs. (1) and (5), the transfer function, $G(s)$, of the WFU between $V_m(s)$ and I_w can be obtained as follows:

$$G(s) = \frac{I_w(s)}{V_m(s)} = \frac{1}{K_c}\left[\frac{W_f(s)}{V_m(s)} + \frac{\Delta G(s)}{V_m(s)}\right] \tag{6}$$

$$G(s) = \frac{I_w(s)}{V_m(s)} = \frac{1}{K_c}\left[\frac{b_0}{(s^2 + a_1 s + a_0)} + \Delta G_d\right] \tag{7}$$

where $\triangle G_d$ denotes $\triangle G(s)/V_m(s)$.

4.2 Controller design for WFU

PID controllers are the most widely used type of controller in modern industry because of their simple control structure. Nonetheless, the conventional PID controllers do not yield reasonable performance over a wide range of operating conditions because of their fixed gains. To solve this problem, the PID parameters need to be adjusted automatically. A self-tuning fuzzy PID controller is a powerful combination that allows a system to improve the control performance with fast response, minimal overshoot, and greater stability.

Fig. 7 shows a conventional PID controller. The controller signal can be expressed in the time domain as:

$$u = K_p e + K_i \int edt + K_d \frac{de}{dt} \tag{8}$$

$$e = I_s - I_w \tag{9}$$

$$K_i = K_p / T_i \tag{10}$$

$$K_d = K_p T_d \tag{11}$$

where e is the tracking error; T_i and T_d are the integral time coefficient and derivative time coefficient, respectively; and K_p, K_i, K_d are the proportional gain, integral gain, and derivative gain, respectively.

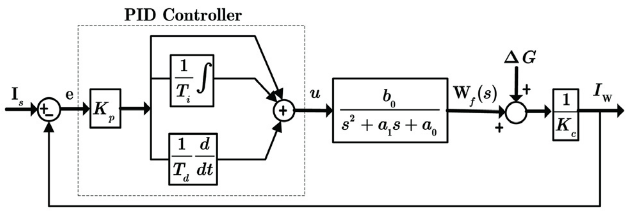

Fig. 7 Conventional PID controller

This paper proposes a self-tuning fuzzy PID controller with two inputs and three outputs. The error, e, and its derivative, $\dot{e}$, are used as inputs. The tuning-gains, K_{tp}, K_{ti}, and K_{td}, are the outputs. The fuzzy controller is added to the conventional PID controller to adjust the parameters of the PID controller.

The new controller is given as follows:

$$u = K_{pf} e + K_{if} \int edt + K_{df} \frac{de}{dt} \tag{12}$$

$$\begin{cases} K_{pf} = 2K_{tp}K_p \\ K_{if} = 2K_{ti}K_i \\ K_{df} = 2K_{td}K_d \end{cases} \tag{13}$$

where K_{pf}, K_{if}, and K_{df} denote the changeable gains of the new controller; K_p, K_i, and K_d are the fixed values from the conventional PID controller; and K_{tp}, K_{ti}, and K_{td} are the tuning-gains from the fuzzy controller.

Fig. 8 shows the proposed self-tuning fuzzy PID controller. K_e and $K_{\triangle e}$ are scaling gains that make the inputs satisfy the operational ranges.

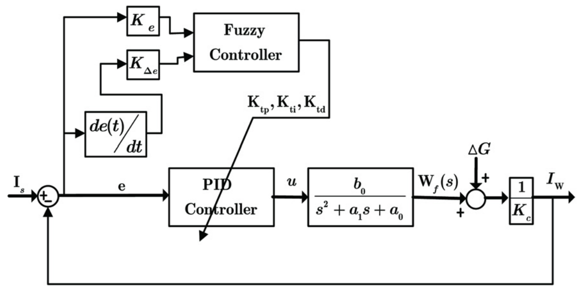

Fig. 8 Self-tuning fuzzy PID controller

The general structure of fuzzy logic control is represented in Fig. 9.

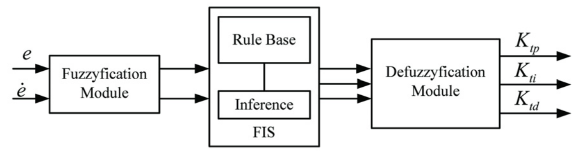

Fig. 9 Fuzzy logic control structure

The inputs range from -1 to 1. For each input variable, five membership functions are used. NB, NS, ZE, PS, and PB are Negative Big, Negative Small, Zero, Positive Small, and Positive Big, respectively. The membership functions of the fuzzy inputs are shown in Fig. 10.

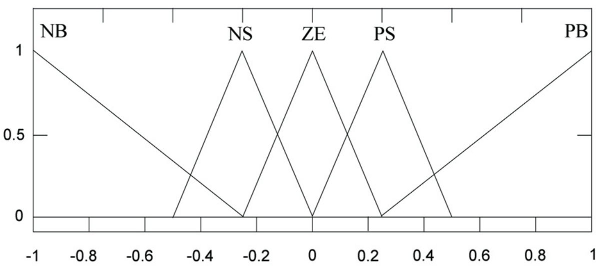

Fig. 10 Membership functions of input (e, $\dot{e}$)

The outputs range from 0 to 1. For each output variable, seven membership functions are used. ZE, MS, S, M, B, MB, and VB are Zero, Medium small, Small, Medium, Big, Medium Big and Very Big, respectively. The membership functions of the fuzzy outputs are shown in Fig. 11.

Using the above fuzzy sets of input and output variables, fuzzy rules are composed as follows:

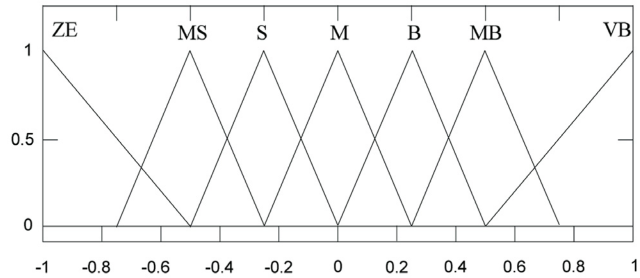

Fig. 11 Membership functions of output (K_{tp}, K_{ti} and K_{td})

Rule i^{th}: If e is A_i and $\dot{e}$ is B_i, then K_{tp} is C_i, K_{ti} is D_i, and K_{td} is E_i, where A_i and B_i are the linguistic label inputs and C_i, D_i, and E_i are the linguistic label outputs. Tables (1)-(3) show the control rules used for the proposed self-tuning fuzzy PID controller.

Table 1 Rule bases for determining gain K_{tp}

$\dot{e}/e$	NB	NS	ZE	PS	PB
NB	VB	VB	VB	VB	VB
NS	B	B	B	MB	VB
ZE	ZE	ZE	MS	S	S
PS	B	B	B	MB	VB
PB	VB	VB	VB	VB	VB

Table 2 Rule bases for determining gain K_{ti}

$\dot{e}/e$	NB	NS	ZE	PS	PB
NB	M	M	M	M	M
NS	S	S	S	S	S
ZE	MS	MS	ZE	MS	MS
PS	S	S	S	S	S
PB	M	M	M	M	M

Table 3 Rule bases for determining gain K_{td}

$\dot{e}/e$	NB	NS	ZE	PS	PB
NB	ZE	S	M	MB	VB
NS	S	B	MB	VB	VB
ZE	M	MB	MB	VB	VB
PS	B	VB	VB	VB	VB
PB	VB	VB	VB	VB	VB

In this paper, the "centroid" method is used for defuzzification to obtain K_{tp}, K_{ti}, and K_{td}. As a result, the rule sets are established and shown on the surfaces in Fig. 12.

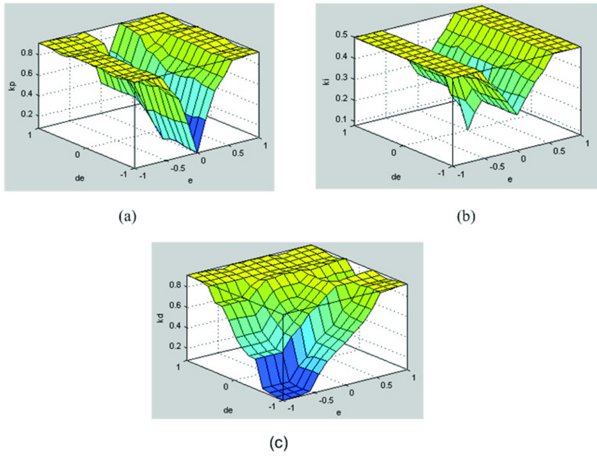

Fig. 12 Rule surface views: (a) K_{tp}, (b) K_{ti}, and (c) K_{td}

5. Simulation and experimental results

5.1 Configuration of hardware

The developed fully automatic GMAW system is presented in Fig. 13.

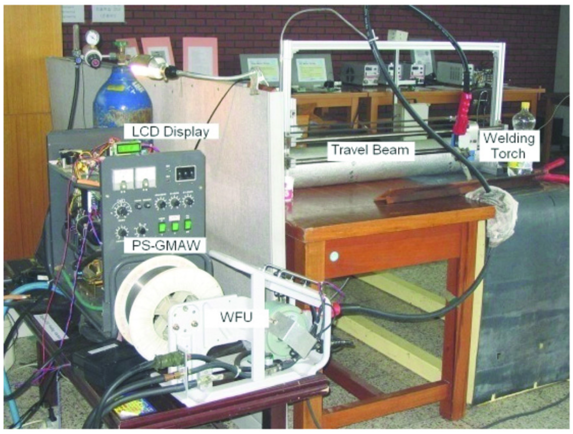

Fig. 13 Developed GMAW system.

It includes the GMAW and a travel beam. The travel beam moves the welding torch along the welding line at a constant velocity. The PS-GMAW has an LCD display and analog display to show the welding current and welding voltage, making it easy to compare the digital and analog values.

5.2 Identification of parameters for transfer function

The transfer function in Eq. (1) can be rewritten as follows:

$$G_m = \frac{W_f}{V_m} = \frac{\omega_{motor} \times b'}{V_m} = \frac{b' k_T}{(L_{am}s + R_{am})(J_m s + b_m) + k_e k_T} \tag{14}$$

$$G_m = \frac{b' k_T}{L_{am} J_m s^2 + (L_{am} b_m + R_{am} J_m) s + (R_{am} b_m + k_e k_T)} = \frac{b_0}{s^2 + a_1 s + a_0} \tag{15}$$

where k_T, k_e, L_{am}, and J_m are the motor torque constant, back electromotive force constant, armature inductance of DC motor, armature resistance, and moment of inertia, respectively. The parameters of the DC motor are given in Table 4.

Table 4 Numerical values of DC motor of WFU

Parameters	Values	Units
k_e	57.3×10^{-3}	V_s/rad
k_T	4.8×10^{-2}	$N\times m/A$
R_{am}	1.1	Ω
L_{am}	0.9×10^{-3}	H
J_m	0.157×10^{-4}	kgm^2
b_m	0.1	N_{ms}

For the specific WFU, gear box rate K_{gear}=1/34, while feed roll diameter D_{roll}=40×10^{-3}m. The ratio between the electrode feed-rate and angular velocity of the DC motor is given as:

$$b' = \frac{W_f}{\omega_{motor}} = \frac{D_{roll}}{2} \times K_{gear} \times 60 = 0.0353 \tag{16}$$

The parameters of transfer function $G_m(s)$ can be calculated as follows:

$$b_0 = \frac{b' k_T}{L_{am} J_m} = 141{,}542 \tag{17}$$

$$a_1 = \frac{L_{am} b_m + R_{am} J_m}{L_{am} J_m} = 7{,}077 \tag{18}$$

$$a_0 = \frac{R_{am} b_m + k_e k_T}{L_{am} J_m} = 7{,}979{,}476 \tag{19}$$

The nominal mathematical model of transfer function $G_m(s)$ is as follows:

$$G_m(s) = \frac{141{,}542}{s^2 + 7{,}077 s + 7{,}979{,}476} \tag{20}$$

The value of K_i depends on the diameter of the welding electrode. Based on the experimental results, the gain, K_i, can be approximated as falling in the range of 0.041~0.046 for a 1.2 mm aluminum electrode. In this paper, K_i=0.043 is chosen.

5.3 Simulation and experimental results

To verify the effectiveness of the proposed controllers, a simulation and experiment were performed for the developed GMAW system shown in Fig. 13. A comparison is presented of the conventional PID and self-tuning fuzzy PID for controlling the wire feed speed of the WFU. Fig. 14 shows the simulation responses for the step type of current for both controllers without disturbance ($\triangle G_d$=0). The parameter values set for the conventional PID (K_p=2, K_i=0.1, and K_d=0.8) and the scaling gains (K_e=2 and $K_{\triangle e}$=0.1) were obtained from experiments with the real model. The control performance of the system using the self-tuning fuzzy PID was better than that using the conventional PID with regard to, not only the rising time, but also the overshoot, settling time, and steady error. Fig. 15 shows how the tuning-gains, K_{tp}, K_{ti} and K_{td}, vary online with the output of the system. After 2 s, the tracking error goes to zero; therefore, the tuning-gains become constant.

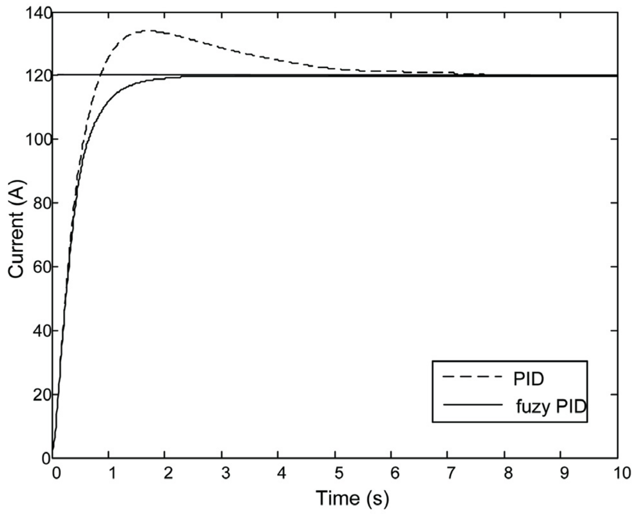

Fig. 14 Simulation response on step type of current in both controllers

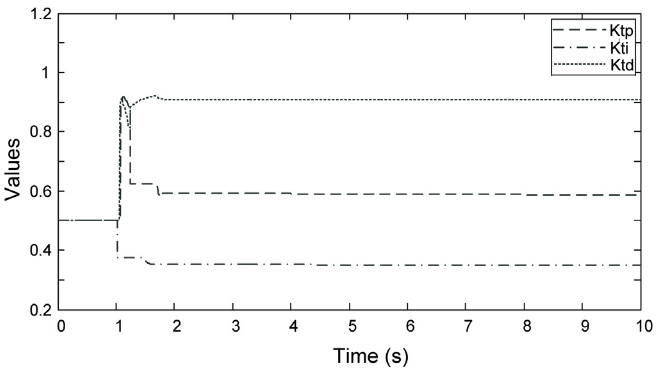

Fig. 15 Tuning-gains, K_{tp}, K_{ti} and K_{td}

Next, to prove the effectiveness of the proposed controller, a disturbance scheme is included. The disturbance generated in this case is given as:

$$\Delta G = A\sin(\omega t) + Rnd(t) \tag{21}$$

where A=2, ω=2π/8, and $Rnd(t)$ is the white noise signal.

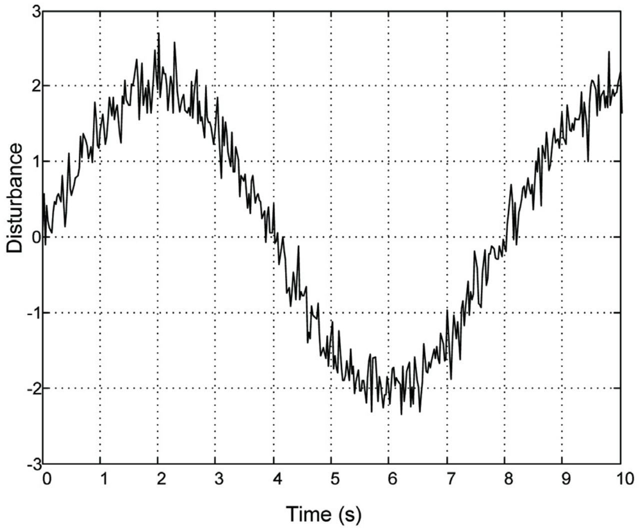

Fig. 16 Disturbance applied to GMAW system.

Fig. 16 shows the disturbance signal, and Fig. 17 shows the output responses in a comparison between the self-tuning fuzzy PID controller and the conventional PID controller. In Fig. 17, the current output is bounded at around 120 ± 5 A with the self-tuning fuzzy PID controller and around 120 ± 20 A with the conventional PID controller. It is obvious that the proposed controller achieves the better tracking response. Fig. 18 shows the tuning-gains, K_{tp}, K_{ti} and K_{td}, considering disturbance. After 2 s, the tracking error is bounded at around zero but is not equal to zero; therefore, the tuning-gains still vary.

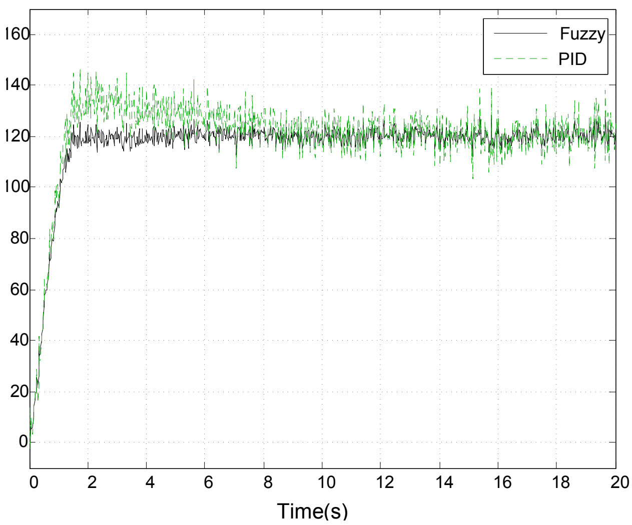

Fig. 17 Simulation results for developed GMAW with disturbance.

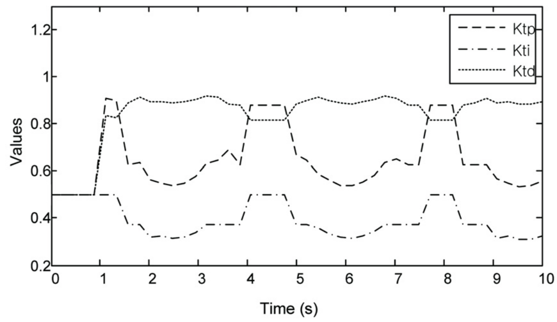

Fig. 18 Tuning-gains, K_{tp}, K_{ti} and K_{td}, with disturbance.

The experimental results for the welding current and voltage are shown in Fig. 19. These results show that the output values are stable and track the setting values very well during the welding process. Fig. 20 (a) and Fig. 20 (b) show welding results for the proposed system and the previous system (Chu and Tung 2005), respectively. These results show that the proposed system's performance is better than the previous system's.

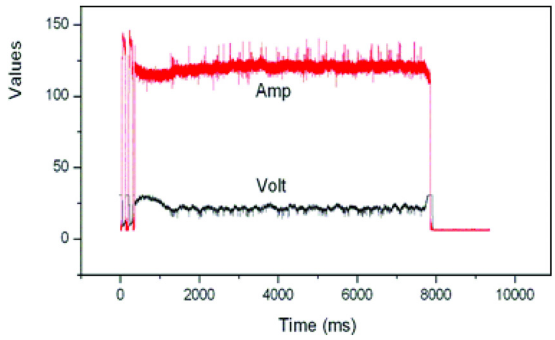

Fig. 19 Experimental results for developed GMAW.

(a) Proposed system result

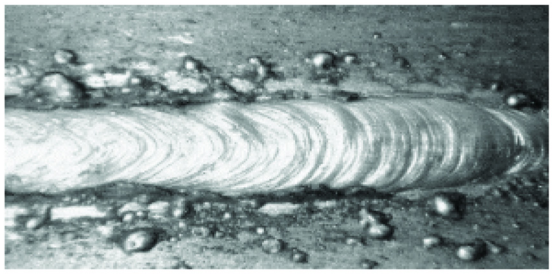

(b) Previous paper result (Chu and Tung 2005)

Fig. 20 Welding results for GMAW.

6. CONCLUSION

This paper presented a new method for developing a digital GMAW system. The PS-GMAW is a constant voltage power supply. The schematic of the PS-GMAW was given. Its controller was based on the incorporation of a microcontroller and IC TL494. A constant arc current was maintained by controlling the wire-feed speed. A self-tuning fuzzy PID controller was developed and successfully applied to the WFU. A simulation and experiment were carried out to evaluate the effectiveness of the proposed control method for the GMAW system. The simulation and experimental results showed that the self-tuning fuzzy PID could achieve good tracking in comparison with the conventional PID controller.

7. ACKNOWLEDGEMENT

This work is a result of a "Human Resource Development Center for Economic Region Leading Industry" project, supported by the Ministry of Education, Science & Technology (MEST) and the Nation Research Foundation of Korea(NRF).

8. REFERENCES

American Welding Society Inc. (1997). Welding HandBook

Abdelrahman M.A. (1998). "Feedback Linearization Control of Current and Arc Length in GMAW Systems," In proceedings of the American control conference, Vol 3, pp 1757-1761.

Chu W.H. and Tung P.C. (2005). "Development of an Automatic Arc Welding System Using a Sliding Mode Control," J. Mach. Tools Manuf., Vol 45, pp 933-939.

Kam B., Cho S. and Kim S.B. (2002). "A Study on Bead Height Control of GMAW by Short Circuit Time Ratio," Journal of Ocean Engineering and Technology, Vol 16, No 2, pp 53-59.

Lincoln Electric Company (1997). MIG/MAG Welding Guide for Gas Metal Arc Welding (GMAW), Third ed.

Mohammad M.A. and Mohammad H. (2011). "Welding Current and Arc Voltage Control in a GMAW Process Using ARMarkov Based MPC," Journal of Control Engineering Practice.

Naidu D.S., Ozcelik S. and Moore K.L. (2003). "Modeling Sensing and Control of Gas Metal Arc Welding," Elsevier publications.

Ngo M.D., Duy V.H., Phuong N.T., Kim H.K. and Kim S.B. (2007). "Development of Digital Gas Metal Arc Welding System," Journal of Materials Processing Technology, Vol 189, pp 384-391.

Truong D.Q. and Ahn K.K. (2009). "Force Control for Hydraulic Load Simulator Using Self-Tuning Grey Predictor–Fuzzy PID," Mechatronics, Elsevier, Vol 19, pp 233-246.

Zhang Y.M. and Liu Y.C. (2003). "Modeling and Control of Quasi-Keyhole Arc Welding Process," Control Engineering Practice, pp 1401-1411.

2011년 6월 13일 원고 접수
2011년 12월 15일 심사 완료
2011년 12월 23일 게재 확정